

Modeling serviceability performance and ultimate capacity of corroded reinforced and prestressed concrete structures

Antonio Mari  | Jesús-Miguel Bairán  | Eva Oller  | Noemi Duarte 

Department of Civil and Environmental Engineering, Universitat Politècnica de Catalunya, Barcelona, Spain

Correspondence

Jesús-Miguel Bairán, Department of Civil and Environmental Engineering, Universitat Politècnica de Catalunya, Campus Nord Jordi Girona 1-3, C-1 201, 08034 Barcelona, Spain.
Email: jesus.miguel.bairan@upc.edu

Funding information

Ministerio de Ciencia e Innovación, Grant/Award Number: RTI2018-097314-B-C21

Abstract

Corrosion reduces the area of reinforcement steel, affects its mechanical properties, the bond properties, and produces concrete cracking. Thus, reduction of the bearing capacity and stiffness, increments of deflections and redistribution of stresses and internal forces, in statically indeterminate structures, take place. In addition, the efficiency of strengthening systems of corroded structures depends on their state of stresses, strains and damage previously to strengthening. In this paper, a nonlinear and time dependent step by step analysis model for reinforced and prestressed concrete frames is presented. The model is capable of capturing the structural effects of corrosion and the effects of strengthening interventions, necessary to adequately assess corroded and strengthened structures. Several cases of corroded and strengthened structures are analyzed and the results discussed.

KEYWORDS

assessment, corrosion, numerical modeling, prestressed concrete, reinforced concrete, strengthening, structures

1 | INTRODUCTION

Corrosion of steel is one of the most frequent and relevant deterioration processes suffered by reinforced concrete structures. Steel corrosion causes a reduction of the reinforcement area, changes in the reinforcing bars mechanical properties¹ and loss of bond properties between steel and concrete.^{2,3} In addition, volumetric expansion of corrosion products causes splitting stresses along corroded reinforcement, leading to cracking and eventually spalling of the

cover. As the reinforcement becomes more exposed, the corrosion rate increases, accelerating the deterioration process.⁴ As a consequence of these phenomena, a reduction in the service performance and strength takes place.

When a statically determinate structure undergoes steel corrosion, the reduction of steel area in the most corroded region may result in the formation of a plastic hinge and eventually evolve into a collapse mechanism. However, statically indeterminate structures, due to their redundancy, have the capacity to redistribute internal forces between the most and the least damaged regions, so that the formation of a plastic hinge does not necessarily lead to structural collapse.⁵ As a consequence, they are more capable to accommodate the effects of higher corrosion levels than statically determinate structures. However, the capacity of internal

Discussion on this paper must be submitted within two months of the print publication. The discussion will then be published in print, along with the authors' closure, if any, approximately nine months after the print publication.

This is an open access article under the terms of the Creative Commons Attribution-NonCommercial-NoDerivs License, which permits use and distribution in any medium, provided the original work is properly cited, the use is non-commercial and no modifications or adaptations are made.

© 2021 The Authors. Structural Concrete published by John Wiley & Sons Ltd on behalf of International Federation for Structural Concrete.

forces redistribution and the higher stiffness associated with redundant structures (i.e., continuous vs. simply supported bridge decks) can hide the actual level of damage of the structure in such a way that it might not be adequately estimated by visual inspections.

In prestressed concrete (PC) structures, the high stress level in the tendons radically modifies the steel corrosion process. The stress corrosion is characterized by the coupling between the conventional corrosion (pitting attacks in chloride environment) and the steel micro-cracking, the latter induced by the high stress level and hydrogen embrittlement.⁶ Consequently, for a low corrosion level of the tendon and under normal service loading, the steel micro-cracking can lead to brittle failure. However, studies regarding the structural response of PC structures affected by corrosion are still rather limited, if compared to the literature about corroded RC elements.^{7,8}

Many corroded structures must be strengthened in order to ensure the required levels of serviceability and safety along their service life. For this purpose, it is necessary to realistically assess the structural response before and after the intervention. The capacity and serviceability performance of the strengthened structure depend on the previous state of stresses, strains, cracks and, in general, the existing damage. Therefore, sequential step by step non-linear analysis models, accounting for the load, time history, evolution of materials properties, structural scheme and boundary conditions, may become very helpful for simulating the effects of deterioration, repair and strengthening operations, and therefore for assessing the efficiency of the strengthening system.

In this paper, an extension of a previously developed nonlinear analysis model developed by Mari⁹ is presented to consider in a simplified way the deterioration effects due to corrosion of steel and the effects of different types of strengthening operations. Comparisons between the results predicted by the model with those experimentally measured in corroded beams are presented. In addition, two theoretical examples of corroded and strengthened concrete beams are presented, to show the capabilities to capture the complex phenomena that take place in corroded structures and the efficiency of the strengthening systems proposed.

2 | NUMERICAL SIMULATION OF THE STRUCTURAL EFFECTS OF CORROSION AND STRENGTHENING

2.1 | Brief description of the analytical model

The previously developed non-linear and time-dependent analysis model CONS⁹ for 3D concrete frames was modified

to include the effects of steel and concrete deterioration due to the corrosion phenomenon and to simulate the effects of strengthening operations. A filament beam element (Figure 1) with arbitrary cross-section and 13 degrees of freedom is used by the model together with non-linear constitutive equations for the reinforcing and prestressing steel and for the concrete filaments, to account for the non-linear response under increasing loading levels.

The model can take into account the material and geometrical non-linearities as well as the time effects due to creep, shrinkage and relaxation of prestressing steel. Creep strain of concrete is evaluated by an age dependent integral formulation based on the principle of superposition, using a Dirichlet series as creep function. A time step-by-step procedure is carried out in which increments of displacements, strains and other structural quantities are successively added to the previous totals as we march forward in the time domain. Construction steps are defined in which changes in geometry, loads and boundary conditions can take place. The time interval between construction steps is divided into time steps. At each time step, the structure is analyzed under the external applied loads and under the imposed deformations originated during the previous time interval. Iterative procedures using load or displacement control, combined with

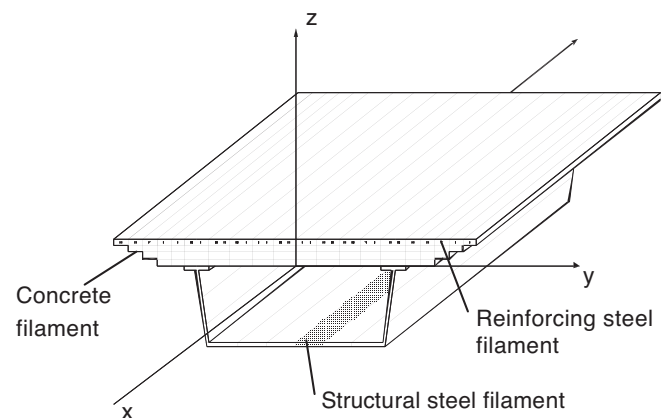


FIGURE 1 Filament reinforced concrete beam element

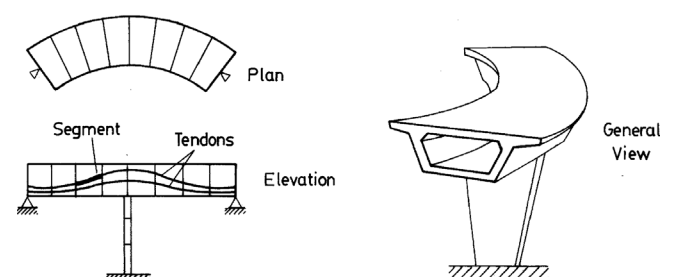


FIGURE 2 Prestressed filament beam element

incremental analyses are used to trace the structural response along the structure service life throughout the elastic, cracked and ultimate load levels. The capacity of the model to capture the time-dependent effects of segmental construction was experimentally checked by Marí and Valdés.¹⁰ Post-tensioning tendons can have a straight or parabolic layout, see Figure 2.

When stressing the tendons, the equivalent prestressing forces obtained by equilibrium of the tendons are applied over the structures. Once the tendons are bonded by grouting the ducts, their deformation follow that of the concrete so that under applied external loads, variations of strains at any point of the prestressing tendons take place and are captured by the model. Then, variations of stresses (after subtracting the relaxation losses) and tendons force are evaluated along the elapsed time. Then, the prestressing loads are updated and the new system of non-linear equations is set.

The incremental and iterative procedure strategy implemented allows tracing the structural response under the elastic, cracked and ultimate ranges up to failure. Most modifications that may take place during the construction process and along the service life, such as deterioration of materials areas and properties, changes in the longitudinal and cross sections geometry, structural scheme, material properties and applied loads, can be simulated by the model, through a step by step solution scheme, as explained next.

2.2 | Simulation of steel corrosion effects

Corrosion of steel produces a loss of area of the affected bar or wire, and, consequently, a loss of flexural capacity and stiffness of the reinforcement and, in prestressed structures, a loss of the prestressing force. Furthermore, in the case of pitting corrosion, non-symmetric loss of area of bars with different properties in the inner and outer layers (i.e., ferrite-perlite and martensite), changes in the effective reinforcing bars properties (yield stress, ultimate stress and strain or modulus of elasticity) also take place.

The non-linear analysis model CONS was modified to reproduce the reduction of the reinforcement steel area in ordinary bars and in prestressing wires.^{11,12} It should be noticed that corrosion induced by carbonation and chlorides contamination tend to be of the type uniform and pitting, respectively. Both types of corrosion can be simulated as progressive loss of area, by considering different effective areas loss. The modifications of the bars or strand properties due to corrosion have not been included in the model for the time being. The loss of steel area due to corrosion is estimated through the following equation:

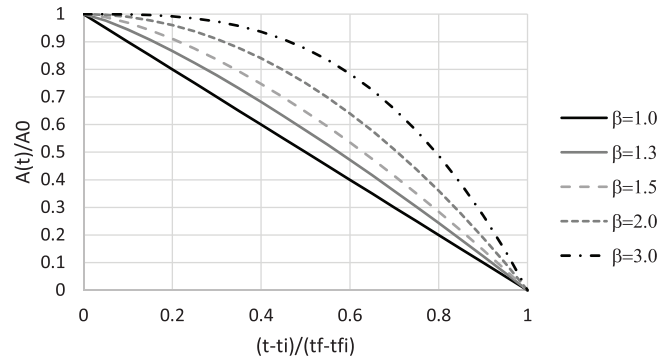


FIGURE 3 Different acceleration area loss simulated by Equation (1) for different values of β

$$A(t) = A(t_0)[1 - D_c(t)] = A(t_0) \left[1 - \left(\frac{t - t_i}{t_f - t_i} \right)^\beta \right] \quad (1)$$

where $A(t_0)$ is the initial area of steel, t is the elapsed time since the initiation of the corrosion, t_i is the instant of the initiation of the corrosion and, t_f is the instant when the steel is totally corroded, so that $A(t_f) = 0$. $D_c(t)$ is a function defining the time evolution of the damage and β is an exponent related to the corrosion rate. For $\beta = 1$, the reduction of steel area occurs at a constant time rate, while for $\beta > 1$ and $\beta < 1$ the area reduction accelerates or decelerates, respectively. As can be seen in Figure 3, this area degradation model can be fitted to reproduce the influence of the bar size on the rate area reduction, or the increase of rate after cracking or loss of cover.

Similarly, an increase in the volume of corrosion products (rust) can cause concrete to crack, and eventually to spall off the cover. Thanks to the evolutionary capabilities of the model, this phenomenon can be considered as well by elimination of one or more concrete layers at specified times. The exact moment in which concrete spalling takes place is generally uncertain and shows great variability. However, it is accepted that the starting point of losing of concrete cover may be considered when the attack penetration (chlorides or carbonation) reaches the value for crack initiation (P_{x0})¹³; the time of cover spalling is, therefore, bigger or equal to the moment reaching this penetration. The attack penetration that initiates cracking may be estimated as in Equation (2); where $\frac{c}{\phi}$ is the cover to diameter ratio and $f_{c,sp}$ is the splitting resistance in MPa.

$$P_{x0} = \left(83.8 + 7.4 \frac{c}{\phi} - 22.6 f_{c,sp} \right) 10^{-3} \geq 0 \quad (2)$$

The loss of steel area results in a reduction in capacity and in stiffness of any cross section affected by corrosion.

Thus, when performing the computation of internal forces, by integration of the stresses at the sections placed at the element's Gauss points, the external forces will not be balanced by the internal ones. Then, these unbalanced forces are automatically introduced in the non-linear iterative scheme, until equilibrium is obtained. As a consequence of corrosion, increments of stresses and strains in concrete and steel, increments of deflections (due to the loss of stiffness) and redistribution of internal forces takes place to satisfy equilibrium and compatibility conditions for the current state of the materials.

2.3 | Simulation of the structural effects of strengthening

Along the time step by step procedure, the numerical model allows introducing changes in most parameters and conditions affecting the structural behavior along the entire service life. Such changes may be related to the section geometry, longitudinal structural scheme, support conditions, materials properties, reinforcement areas, prestressing areas and forces, links between elements, applied loads and imposed deformations. Thus, the following situations related to remodeling and strengthening of structures can be simulated: substitution of damaged concrete parts, enlargement of concrete cross section, placement of new reinforcement bars, steel plates or bonded FRP laminates, placement or removal of temporary shores, imposed movements, blocking of pins, monolithically connect elements and application of external prestressing, among others.^{14,15}

With this scheme, the response of structures before and after the strengthening can be obtained, including the effects of previous damage and those of the repair, retrofit or strengthening operations.

3 | VERIFICATION OF THE MODEL

3.1 | Simulation of experimental test on a simply supported post-tensioned concrete beam with cutted wires to reproduce pitting corrosion effects

An experimental campaign was carried out to study the structural effects of the loss of steel area in a post-tensioned tendon of eight strands of 140 mm^2 each, to simulate effects of pitting corrosion.¹⁶ For this purpose, four simply supported post-tensioned beams of 8 m total length and 7.5 m span length were tested under a concentrate load until failure. After prestressing the cables, the effect of the loss of steel area in the tendon was simulated by introducing by means of a mechanical cut in one of the wires. This cut was made in four of the eight strands. The experimental response was monitored through the evolution of strain using fiber optic strain gauges attached to the unaffected wires. Two beams were casted with a parabolic tendon profile, while the tendon profile of the other two was straight, as seen in Figure 4.

Concrete design strength was $f_c = 35 \text{ MPa}$. A rectangular opening was made in one of the sides of the beam, at mid-span section of all the specimens tested, in order to have easy access to the duct and strands.

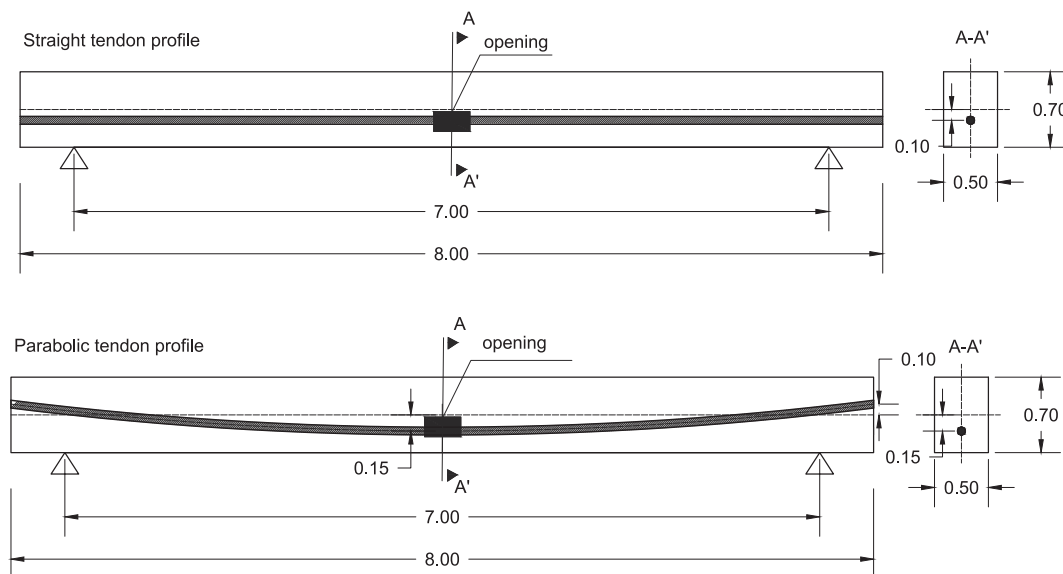


FIGURE 4 Beams subjected to simulated pitting corrosion,¹⁶

The tendon eccentricity in the beams with parabolic profile was 0.15 m in the downward direction in the mid-span, and 0.10 m in the upward direction at the edge of the specimens (Figure 3a). The tendon eccentricity in the specimens with straight profile was 0.10 m.

Figure 5 shows longitudinal and transversal mild reinforcement used for all the specimens.

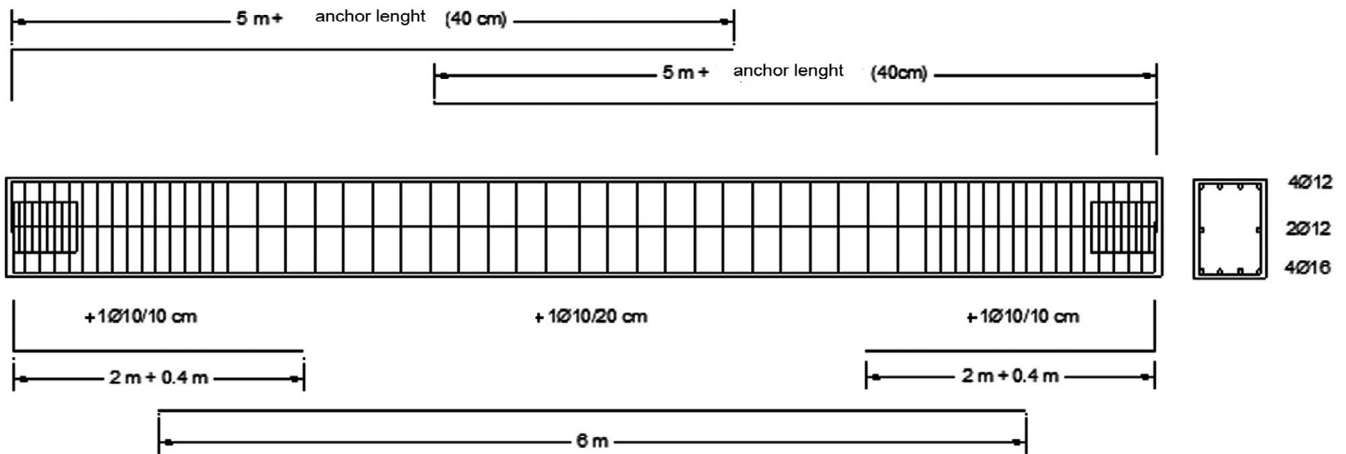
The specimens were post-tensioned at 14 days after concrete casting, with a jacking stress of 1450 MPa. The wedge penetration was reported as 5 mm and the friction and wobble coefficients are $\mu = 0.21$ and $K/\mu = 0.006$ 1/m, respectively. The long-term relaxation was estimated as 8%.

Figure 6 shows the fiber optic sensors and strain gauges glued to the unaffected wires. Afterwards, all the specimens were tested until failure under 3-point load test.

3.2 | Comparison between the predicted and the experimental results

In order to validate the model, the numerical simulation of beam V2, with a parabolic tendon layout is performed (Figure 7). The effect of loss of steel area produced by pitting corrosion was simulated by mechanical cutting a

MILD REINFORCEMENT



ANCHOR CUP REINFORCEMENT

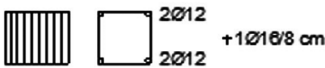


FIGURE 5 Beams passive reinforcement,¹⁶

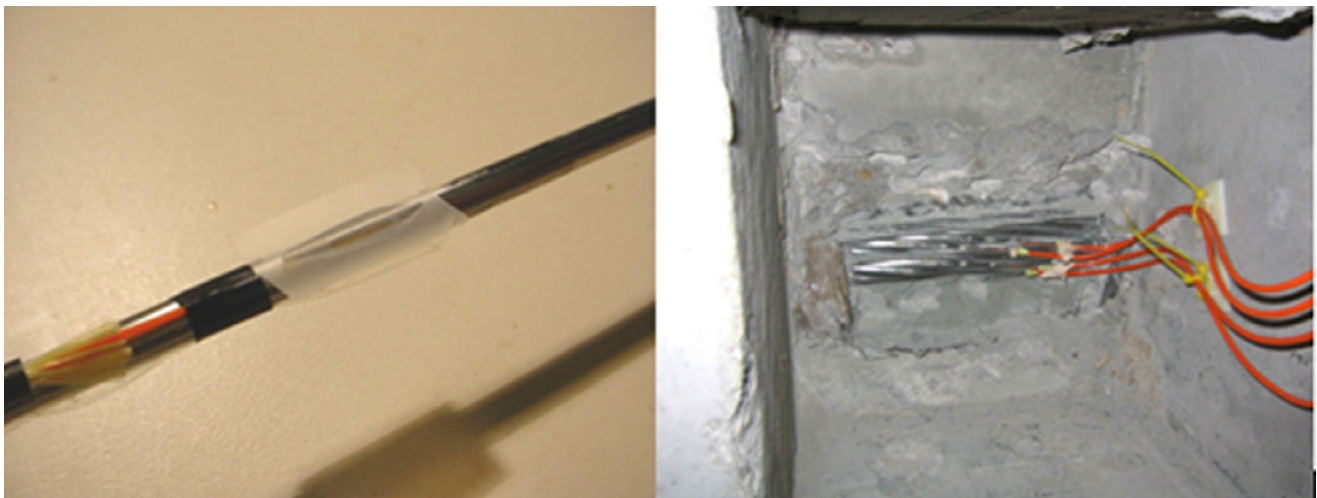


FIGURE 6 Fiber optic sensors,¹⁶



FIGURE 7 Monitoring of the strands of the post-tensioned concrete beam tested,¹⁶

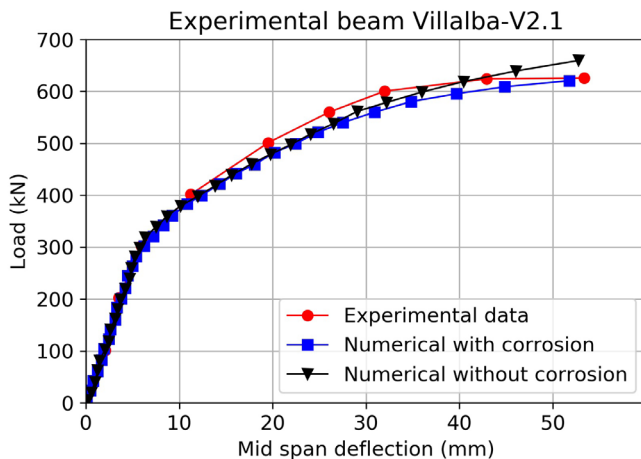


FIGURE 8 Experimental and numerical load-displacement curves

wire in four strands, that is, 4 out of the 8 strands of 7 wires ($A_{pi} = 140 \text{ mm}^2$), were affected by pitting corrosion.

All the experimental phases were reproduced with the numerical model. Firstly, prestressing load and dead weight is applied after 14 days. Then, time effects, that took place until the day of the load test, carried out at the age of 31 days for this specimen, were simulated. Finally, an incremental point load is introduced until failure.

Figure 8 shows a comparison of the load-displacement curves obtained both experimentally and numerically, in two cases: taking into account and neglecting the loss of area. Good agreement is observed, particularly in the prediction of the failure load; which was 625 kN in test, while

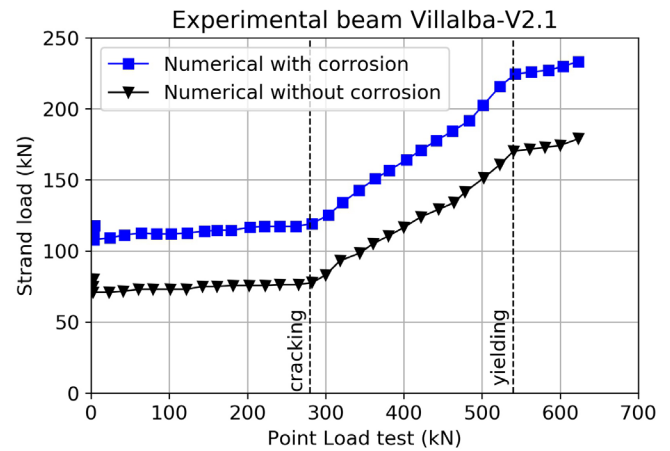


FIGURE 9 Force at strands affected and not affected by pitting

the model prediction was 620 kN, which implies a difference of 0.8%. Similarly, the elastic stiffness of the experiment and the numerical prediction are almost the same. However, the numerical model slightly over predicts the post-cracking deflection. On the other hand, if the effect of pitting corrosion is not considered in the model, the predicted failure load is 660 kN, which is a difference of 5.6% with respect to the experimentation and the model considering strand pitting.

Figure 9 shows the evolution of the strand force for the units affected by the pitting corrosion and the intact ones. It can be seen that the corroded strands develop less force because of the loss of steel area.

An important increment of the strand force is observed after the cracking is produced for a load of 280 kN. For a point load of 540 kN, yielding of the active reinforcement occurs; however, the beam shows additional increment of load capacity as some of the longitudinal passive bars are still in elastic range. The maximum load capacity is reached after yielding of both passive and active reinforcement.

4 | ANALYSIS OF A RC PEDESTRIAN BRIDGE SUBJECTED TO STEEL CORROSION

A three-span continuous reinforced concrete pedestrian bridge is analyzed in this section. The structure is located in a marine environment, and is affected by corrosion of the bottom layer of reinforcement.¹⁷ The geometry and reinforcement of the bridge is shown in Figure 10. The concrete and steel strengths are $f_c = 30 \text{ MPa}$ and $f_y = 500 \text{ MPa}$, respectively. The loads acting on the structure are its self-weight ($SW = 70 \text{ kN/m}$), a dead load ($DL = 10 \text{ kN/m}$), and a live load ($LL = 52 \text{ kN/m}$). It is

assumed that, at the age of 28 days, the structure is subjected to the total nominal load, as a result of a load test previous to service situation. Afterwards, the structure is unloaded to the level of quasi-permanent loads ($SW + DL + 0.4LL = 100.8 \text{ kN/m}$), that is maintained constant until the time of corrosion initiation. During this phase, the effects of creep, shrinkage and relaxation take place. The initiation of corrosion takes place at 1000 days at a corrosion rate of $2 \cdot 10^{-3} \text{ mm/day}$. It is assumed that spalling of the bottom concrete takes place at 2000 days. In order to study the evolution of the structure carrying capacity with the corrosion degree, an incremental analysis up to failure under a distributed load along the whole

bridge length was made at different instants, after construction of the bridge.

Figure 11a shows the evolution of the midspan deflection with time, with and without corrosion, as a function of the degree of corrosion. As the reinforcement area reduces and the cover is lost, the deflections increase considerably. In the same figure, the effects of a repair carried out at 4300 days is shown. The repair consists of protecting the bars and replacing the concrete cover to stop the progression of corrosion. It can be seen that, even though no additional reinforcement is added, deflections remain almost constant, probably due to the fact that almost all creep and shrinkage

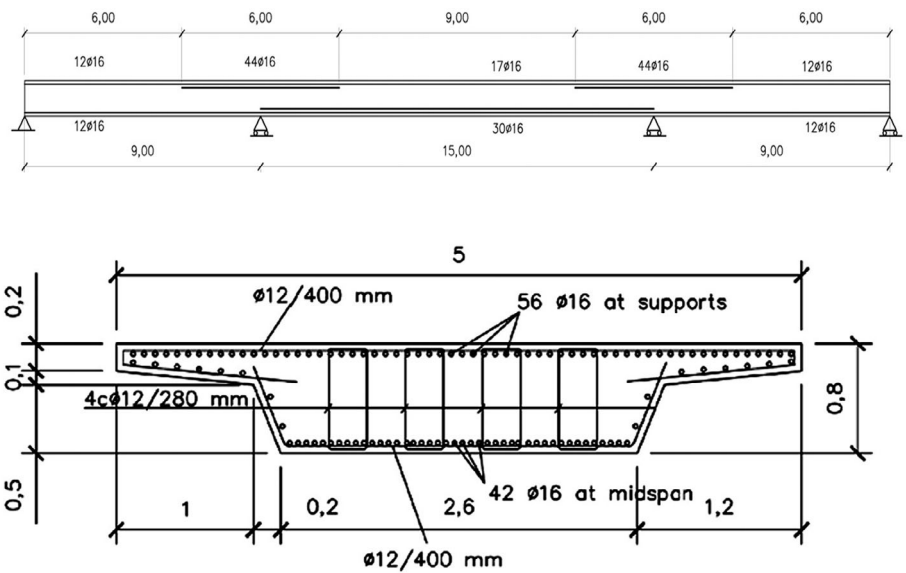


FIGURE 10 Geometry and reinforcement of the structure analyzed

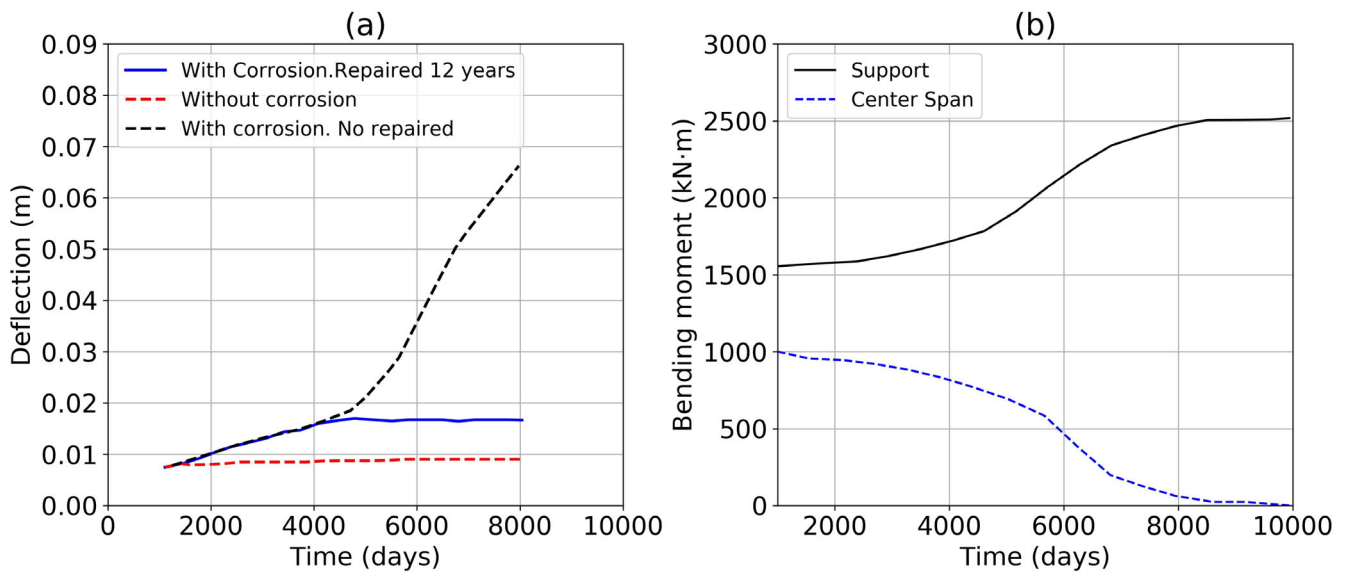


FIGURE 11 (a) Evolution of deflection with time. (b) Evolution of bending moments

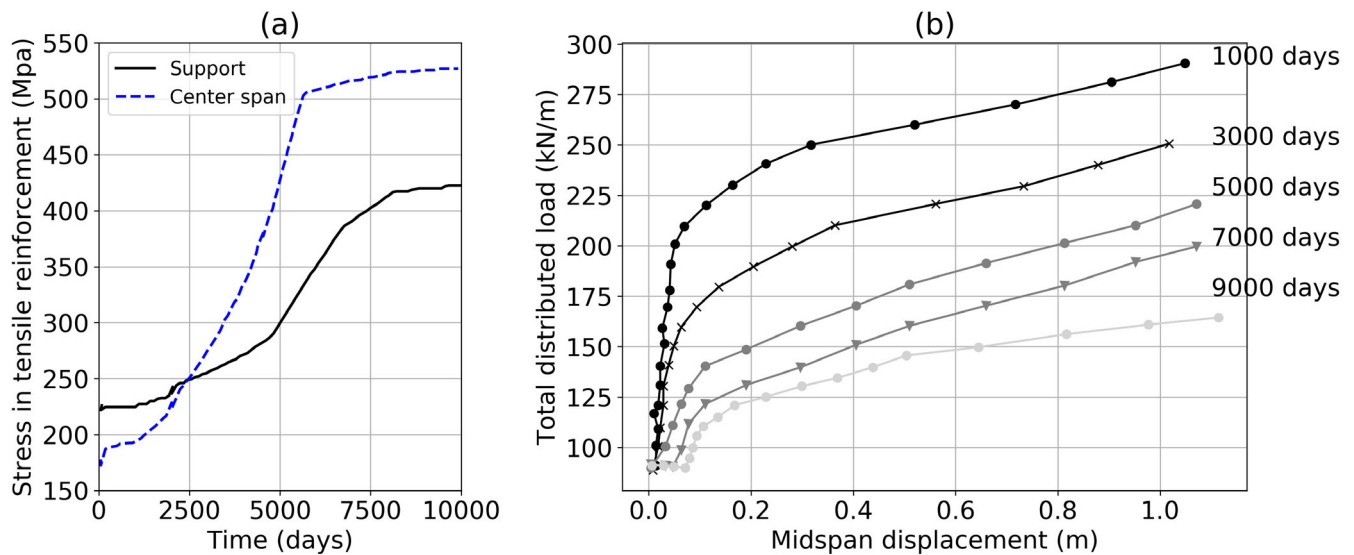


FIGURE 12 (a) Evolution of reinforcement stresses. (b) Load–displacement for different corrosion levels

have already taken place, the cracks have been sealed and the concrete cover has been restored, so that no further loss of steel and increments of crack widths take place.

Figure 11b shows the evolution with time of the bending moments at the support and at the bridge midspan. It can be observed that a redistribution of bending moments due to the materials deterioration takes place, decreasing the positive bending moment from 1000 kNm up to a very small value; at the same time, the negative moment increases from 1500 to 2500 kNm.

Figure 12a shows the steel stresses at the support and at mid span sections. It is observed that tensile steel stresses at the center span section increase with time, due to the loss of steel section, while the tensile stresses at the support section also increase due to the redistribution of internal forces.

Figure 12b shows the load–displacements–curves for different degrees of corrosion and the ultimate capacity of the bridge, loaded with a distributed load along its entire length. It can be seen that corrosion reduces the total load that can carry the structure. For the case of corrosion initiation at 1000 days, the reduction factors for 3000, 5000, 7000 and 9000 days are 13.8%, 24.2%, 31.0% and 43.0%, respectively.

5 | CONCLUSIONS

Corrosion of steel reinforcement produces local effects as well as changes in the overall response of a structure. In addition, the efficiency of a strengthening intervention depends, among other factors, on the previous state of

strains, stresses and damage of the structure. Nonlinear analytical models capable of capturing these effects are very adequate to assess deteriorated and strengthened structures.

In this paper an analytical model capable of tracing the structural response of reinforced concrete frames under loads and environmental actions, including deterioration of materials and the effects of strengthening operations, has been presented. The experimentally measured response of a tested post-tensioned concrete beam in which wires have been cut to simulate the structural effects of pitting corrosion, has been simulated with the developed model. Very good agreement has been obtained in the load–displacement curve of the “corroded” beam. Furthermore, the model has shown its capability to provide the increments of stresses, strains, prestressing force and deflections under incremental load in the elastic, cracked and ultimate ranges.

A case study has been carried out to show the capabilities of the model to reproduce the structural effects of reinforcement corrosion and the efficiency of a repair intervention. The structure studied consists of a three span continuous pedestrian bridge with a solid slab cross section, subjected to corrosion of the bottom reinforcement. Redistribution of internal forces, increments of stresses and displacements and reduction of the structure carrying capacity have been consistently captured by the model. Since the model is based on beam-column elements, and its results can be easily interpreted by structural engineers, it is a proper tool for the serviceability and safety assessment of structures along their lifetime.

Further improvements are being currently introduced in the model, such as the effects of corrosion on the

transverse reinforcement, the automatic updating of the steel mechanical properties in the reinforcement due to corrosion and the effects of bond deterioration on the structural behavior.

ACKNOWLEDGMENTS

The present work is part of research project RTI2018-097314-B-C21 funded by the Spanish Ministry of Science, Innovation and Universities through the Spanish Agency of Research (AEI), to whom the authors want to express their gratitude for the financial support received.

DATA AVAILABILITY STATEMENT

The data that support the findings of this study are available from the corresponding author upon reasonable request.

ORCID

Antonio Marí  <https://orcid.org/0000-0002-0994-0715>

Jesús-Miguel Bairán  <https://orcid.org/0000-0003-2831-1479>

Eva Oller  <https://orcid.org/0000-0002-0845-3587>

Noemi Duarte  <https://orcid.org/0000-0002-4542-8487>

REFERENCES

- Fernández I, Bairán JM, Marí A. Corrosion effects, on the mechanical properties of reinforcing steel bars. Fatigue and σ - ϵ behavior. *Construct Build Mater.* 2015;101:772–83.
- Al-Sulaimani G, Kaleemullah M, Basunbul I. Influence of corrosion and cracking on bond behavior and strength of reinforced concrete members. *ACI Struct J.* 1990;87:220–2312.
- Alonso C, Andrade C, Rodríguez J, Díez JM. Factors controlling cracking of concrete affected by reinforcement corrosion. *Mater Struct.* 1998;31:435–41.
- Broomfield J. Corrosion of steel in concrete: understanding, investigation and repair. 2nd ed. Abingdon, UK: Taylor & Francis; 2002.
- Fernández I, Herrador M, Marí A, Bairán J. Structural effects of steel reinforcement corrosion on statically indeterminate reinforced concrete members. *Mater Struct.* 2016;49:4959–73.
- Nürnberg U. Corrosion induced failure mechanisms of pre-stressing steel. *Mater Corros.* 2002;53:591–601.
- Coronelli D, Castel A, Vu NA, François R. Corroded post-tensioned beams with bonded tendons and wire failure. *Eng Struct.* 2009;31:1687–97.
- Recupero A, Spinella N. Experimental tests on corroded prestressed concrete beams subjected to transverse load. *Struct Concr.* 2019;20:2220–9.
- Marí A. Numerical simulation of the segmental construction of three dimensional concrete frames. *Eng Struct.* 2000;22:585–96.
- Marí A, Valdés M. Long-term behaviour of continuous precast concrete girder bridges model. *ASCE J Bridge Eng.* 2000;5:22–30.
- Marí A, Bairán J, Oller E, Fernández I. Numerical simulation of the structural effects of the deterioration in concrete structures. Proceedings FIB Congress “Concrete Structures for Sustainable Community”; 2012 Jun 12–14; Stockholm.
- Marí A, Bairán J, Fernández I. “Numerical modelling of pretressed concrete structures subjected to stress corrosion” (in Spanish). Final report, research project SEDUREC (safety and durability of structures and constructions). Barcelona, Spain: CIMNE, UPC; 2011.
- CONVECTEC. A validated user's manual for assessing the residual service life of concrete structures. EC Innovation Programme IN30902I., CSIC-Instituto Torroja; 1989:152.
- Marí A, Bairán J, Moreno R, Alvarez, JJ. Analysis of remodelled and strengthened concrete bridge structures. Proceedings FIB Congress “Concrete Structures for Sustainable Community”; 2012 Jun 12–14; Stockholm
- Marí A, Bairán JM, Oller E. Assessment of the efficiency of strengthening solutions in concrete structures by means of non-linear step by step analysis models. *Hormigón y Acero.* 2021. <https://doi.org/10.33586/hya.2021.3043>.
- Villalba V. Study on the monitoring of structures subjected to stress corrosion, by means of optical fiber (in Spanish) [unpublished dissertation]. Barcelona, Spain: Polytechnic University of Catalonia; 2004
- Marí A, Bairán J. Evaluation of the response of concrete structures along their service life by nonlinear evolutive analysis methods. 1st International Symposium on Life Cycle Civil Engineering, IALCEE08; 2016 Jun 12–14; Varena, Lake Como, Italy

AUTHOR BIOGRAPHIES



Antonio Marí, MSc, PhD is a civil engineer and professor at Universitat Politècnica de Catalunya, Department of Civil and Environmental Engineering, Campus Nord Jordi Girona 1-3, C-1 201, 08034 Barcelona, Spain. Email: antonio.mari@upc.edu



Jesús-Miguel Bairán, MSc, PhD is a civil engineer and associate professor at Universitat Politècnica de Catalunya, Department of Civil and Environmental Engineering, Campus Nord Jordi Girona 1-3, C-1 201, 08034 Barcelona, Spain. Email: jesus.miguel.bairan@upc.edu



Eva Oller, MSc, PhD is a civil engineer and associate professor at Universitat Politècnica de Catalunya, Department of Civil and Environmental Engineering, Campus Nord Jordi Girona 1-3, C-1 201, 08034 Barcelona, Spain. Email: eva.oller@upc.edu



Noemi Duarte, MSc is a civil engineer and researcher at Universitat Politècnica de Catalunya, Department of Civil and Environmental Engineering, Campus Nord Jordi Girona 1-3, C-1 201, 08034 Barcelona, Spain. Email: noemi.duarte@upc.edu

How to cite this article: Marí A, Bairán J-M, Oller E, Duarte N. Modeling serviceability performance and ultimate capacity of corroded reinforced and prestressed concrete structures. *Structural Concrete*. 2021;1-10. <https://doi.org/10.1002/suco.202100159>